Fast Direction-Finding Algorithm by Partial Spatial Smoothing in Sparse MIMO Radar

Sheng Liu[1], Feng Qin[2], Jing Zhao[1], Weizhi Xiong[1, *], and Ziqing Yuan[1]

Abstract—For reducing the computational complexity of direction-finding algorithm in sparse multiple-input multiple-output (MIMO) radar, a low-complexity partial spatial smoothing (PSS) algorithm is presented to estimate the directions of multiple targets. Firstly, by dealing with a partly continuous sampling covariance vector in PSS technology, an incomplete signal subspace can be obtained. Then, a special matrix can be obtained by using this incomplete signal subspace. Meanwhile the incomplete signal subspace can also be repaired by the special matrix. At last, the multiple signal classification (MUSIC) algorithm is used to obtain direction estimations. In the process of obtaining signal subspace, no eigenvalue decomposition (EVD) needs to be performed. Compared with the traditional spatial smoothing (SS) technology, the proposed algorithm has lower computational complexity and higher estimation accuracy. Many simulation results are provided to support the proposed scheme.

1. INTRODUCTION

Recently, multiple-input multiple-output (MIMO) radar is widely concerned for its advanced performances in enhancing degree of freedom (DOF) and improving resolution. Bistatic MIMO radar and monostatic MIMO radar are two frequently-used radar structures for direction-finding of multiple targets. The receiving array and transmitting array of a bistatic MIMO radar are installed with larger distance. Many direction-finding algorithms [1–6] based on bistatic MIMO radar have been proposed to estimate the directions of departure (DODs) of transmitted signals and directions of arrival (DOAs) of received signals.

The receiving array and transmitting array of a monostatic MIMO radar are placed in close together positions. For each target, the DOD of transmitted signal and the DOA of received signal are approximately equal. In [7], a DOA estimation algorithm based on polynomial-root was proposed, in which root-finding of polynomial was used to avoid the search of spectral peak. In [8], the authors used selection matrix to reduce the dimension of received vector and proposed a reduced-dimensional estimation of signal parameters via rotational invariance techniques (ESPRIT) algorithm. This algorithm shows lower computational complexity and higher estimation precision than SS algorithm. Subsequently, a reduced-complexity Capon algorithm [9] and a two-dimensional (2D) reduced-dimensional ESPRIT [10] were proposed based on the reduced-dimensional technology. In [11], a conjugate ESPRIT algorithm was proposed for non-circular signals and showed advantage in extending virtual aperture. However, for the above algorithms [7–11], both the receiving array and transmitting array are uniform linear arrays, and the utilization efficiency of sensors is limited.

In order to improve the utilization efficiency of sensors and enhance the DOF of MIMO radar, many sparse MIMO radars have been proposed. Co-prime MIMO radars [12, 13] are designed around the co-prime arrays [14, 15], whose both receiving array and transmitting array of are co-prime linear arrays. Because of the sparse structure, co-prime MIMO has higher DOF than uniform radar MIMO.

But compared with co-prime array, nested array [16–18] can provide higher DOF. In [17], using the construction features of nested array [16], a nested MIMO radar [19] with hole-free difference and sum co-array (DSCA) was proposed and had higher DOF than co-prime MIMO radars [12, 13]. In [20], this nested MIMO radar was improved by substituting the nested array [17] into nested array [16], and the DOF was improved further. The critical point for the use of a sparse MIMO radar is to construct an extended covariance matrix. For the sparse MIMO radar [12, 13, 19, 20], SS algorithm [15] is used to construct an extended covariance matrix, and multiple signal classification (MUSIC) algorithm is used to estimate DOA. However, in order to obtain the signal subspace or noise subspace, this process involves EVD which has higher computational complexity.

In this paper, a low-complexity DOA estimation algorithm is proposed to reduce the computational complexity for sparse MIMO radar. The proposed algorithm uses PSS technology to obtain equivalent signal subspace, and no EVD needs to be carried out. Compared with the traditional SS algorithm, the proposed algorithm has two advantages: (1) the proposed algorithm has lower computational complexity; (2) the proposed algorithm has higher estimation precision.

Notation: Symbols $[\bullet]^*$, $[\bullet]^T$, $[\bullet]^H$, $[\bullet]^+$, $\otimes$, and $E[\bullet]$ are conjugate, transpose, conjugate transpose, generalized inverse, Kronecker product, and expectation, respectively. $\mathbf{M}(i:j,:)$ represents the matrix consisting of the ith row to the jth row of $\mathbf{M}$; $\mathbf{M}(:,i:j)$ represents the matrix consisting of the ith column to the jth column of $\mathbf{M}$; and $\mathbf{v}(i:j)$ represents the vector consisting of the ith element to the jth element of $\mathbf{v}$.

2. DATA MODEL

Suppose that a sparse monostatic MIMO radar array consists of an M-element transmitting array and an N-element receiving array. Fig. 1 and Fig. 2 show two recently proposed nested MIMO radars [19, 20] with a 4-element transmitting array and a 4-element receiving array. The position of physical sensors, the non-negative positions of sum co-array (SCA) and DSCA are shown in the two figures, where the unit interval is half-wavelength ($\lambda/2$) of the incident signal.

The transmitting array transmits multiple orthogonal signal waveforms, and the reflected signals
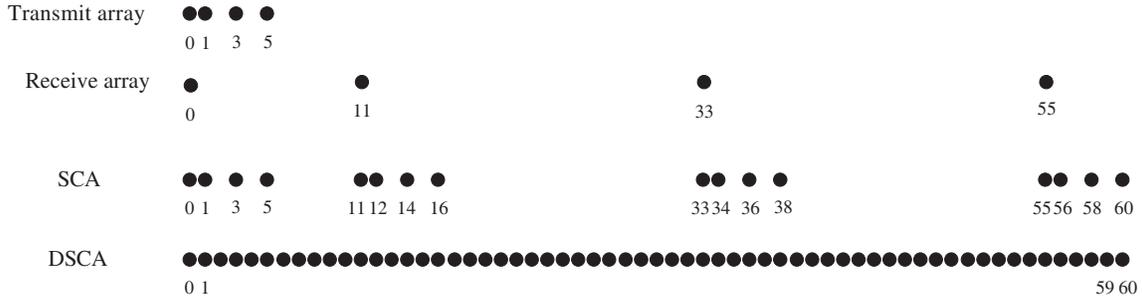

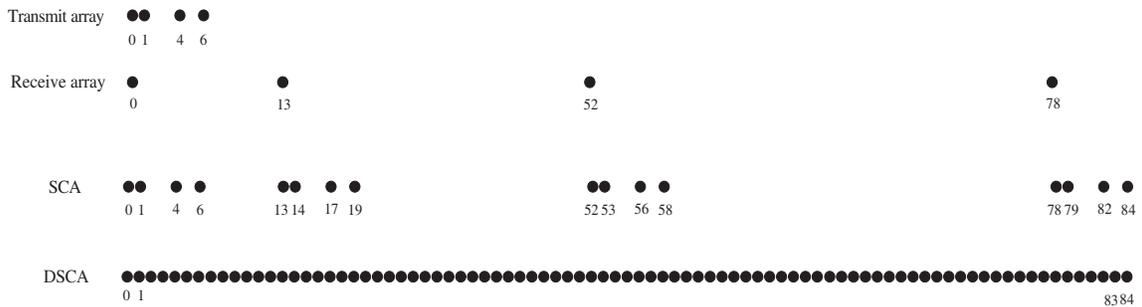**Figure 1.** Construction of nested MIMO radar [19].

Figure 2. Construction of improved nested MIMO radar [20].

from targets are received by receiving array synchronously. $\tilde{d}_m$ is the distance between the first transmitting sensor and the mth transmitting sensor, and d_n is the distance between the first receiving sensor and the nth receiving sensor. Denote the DOA of kth target as θ_k, $k = 1, 2, \ldots, K$, and the output of the matched filter from the receiving array in the tth period can be written as [12, 13]

$$\mathbf{x}(t) = \mathbf{A}(\boldsymbol{\theta})\boldsymbol{\alpha}(t) + \mathbf{n}(t), \quad t = 1, 2, \ldots, T \tag{1}$$

where $\mathbf{A}(\boldsymbol{\theta}) = [\mathbf{a}_r(\theta_1) \otimes \mathbf{a}_t(\theta_1), \mathbf{a}_r(\theta_2) \otimes \mathbf{a}_t(\theta_2), \ldots, \mathbf{a}_r(\theta_K) \otimes \mathbf{a}_t(\theta_K)] \in C^{MN \times K}$, $\mathbf{x}(t) = [x_1(t), x_2(t), \ldots, x_{MN}(t)]^T \in C^{MN \times 1}$, $\mathbf{a}_r(\theta_k) = [1, e^{-\frac{j2\pi d_2 \sin \theta_k}{\lambda}}, \ldots, e^{-\frac{j2\pi d_{N-1} \sin \theta_k}{\lambda}}, e^{-\frac{j2\pi d_N \sin \theta_k}{\lambda}}] \in C^{N \times 1}$, $\mathbf{a}_t(\theta_k) = [1, e^{-\frac{j2\pi \tilde{d}_2 \sin \theta_k}{\lambda}}, \ldots, e^{-\frac{j2\pi \tilde{d}_{M-1} \sin \theta_k}{\lambda}}, e^{-\frac{j2\pi \tilde{d}_M \sin \theta_k}{\lambda}}] \in C^{M \times 1}$, $\alpha = [\alpha_1, \alpha_2, \ldots, \alpha_K]^T$, α_k is the reflection coefficient of the kth target, and $\mathbf{n}(t) = [n_1(t), n_2(t), \ldots, n_{MN}(t)]^T \in C^{MN \times 1}$ is the Gaussian white noise vector with zero mean.

For the proposed data model above, suppose that the reflection coefficient $\alpha_k(t)$ is a random sequence with zero mean. Assume that the element position errors, the mutual coupling effect between elements, and the effect of Doppler frequencies in the orthogonality of signals are ignored.

3. TRADITIONAL SPATIAL SMOOTHING

In this section, we introduce the procedure of traditional spatial smoothing (SS). Suppose that the number of DOFs of a sparse MIMO is $2F + 1$ and that the covariance matrix is denoted as $\mathbf{R}_{xx} = E\{\mathbf{x}\mathbf{x}^H\}$. $2F + 1$ elements with consecutive lags samples are selected from $\mathbf{R}_{xx}$ to construct a covariance vector γ as [19, 20]

$$\gamma = \mathbf{B}\mathbf{P} + \delta_n \mathbf{e} \tag{2}$$

where $\mathbf{B} = [\mathbf{b}(\theta_1), \mathbf{b}(\theta_2), \ldots, \mathbf{b}(\theta_K)] \in C^{(2F+1) \times K}$, $\mathbf{b}(\theta_k) = [e^{\frac{j2\pi dF \sin \theta_k}{\lambda}}, \ldots, e^{\frac{j2\pi \sin \theta_k}{\lambda}}, 1, e^{-\frac{j2\pi \sin \theta_k}{\lambda}}, \ldots, e^{-\frac{j2\pi F \sin \theta_k}{\lambda}}]^T$, $\mathbf{P} = [\, p_1 \quad p_2 \quad \ldots \quad p_K \,]^T \in C^{K \times 1}$ is a vector with $p_k = E\{\alpha_k \alpha_k^H\}$; $\mathbf{e} = [\, 0 \quad \ldots \quad 0 \quad 1 \quad 0 \quad \ldots \quad 0 \,]^T \in C^{(2F+1) \times 1}$ is a vector with only one nonzero element at the $(F + 1)$th position; and δ_n is the power of noise.

Then, using SS algorithm, the extended covariance matrix $\mathbf{R}'_{xx}$ or $\mathbf{R}''_{xx}$ can be constructed by

$$\mathbf{R}'_{xx} = \frac{1}{F+1} \sum_{i=1}^{F+1} \gamma(F + 2 - i : 2F + 2 - i)\gamma^H(F + 2 - i : 2F + 2 - i) \tag{3}$$

or

$$\mathbf{R}''_{xx} = [\, \gamma(F + 1 : 2F + 1) \quad \gamma(F : 2F) \quad \ldots \quad \gamma(1 : F + 1) \,] \tag{4}$$

We can also refer [17–21] to find the detailed procedure of the traditional SS algorithm. According to Eqs. (3) and (4), it is clear that both $\mathbf{R}'_{xx}$ and $\mathbf{R}''_{xx}$ contain noise covariance δ_n. In order to obtain signal subspace or noise subspace, EVD of $\mathbf{R}'_{xx}$ or $\mathbf{R}''_{xx}$ should be performed. Then, the subspace-based approaches such as MUSIC algorithm [22] and ESPRIT algorithm [23] can be utilized to get the estimation of DOA. Of course, we can also deal with the matrix $\mathbf{R}'_{xx}$ or $\mathbf{R}''_{xx}$ by the low-complexity propagator method (PM) [24]. However, the precision of PM algorithm is far lower than MUSIC algorithm and ESPRIT algorithm.

4. PARTIAL SPATIAL SMOOTHING

4.1. Construction of Incomplete Signal Subspace

Just for the existence of noise, SS algorithm needs EVD of covariance to separate signal subspace and noise subspace. Observing the covariance vector γ, we can find that only the $(F + 1)$th element of γ contains noise component. In order to eliminate the impact of noise, we remove the middle element of γ and denote the new vector as

$$\mathbf{r} = \begin{bmatrix} \mathbf{r}_1 \\ \mathbf{r}_{-1} \end{bmatrix} = \begin{bmatrix} \mathbf{B}_1 \\ \mathbf{B}_{-1} \end{bmatrix} \mathbf{P} \tag{5}$$

where $\mathbf{r}_1$, $\mathbf{r}_{-1}$ are the first F rows and last F rows of γ, respectively, and $\mathbf{B}_1$, $\mathbf{B}_{-1}$ are the first F rows and last F rows of $\mathbf{B}$, respectively.

Because of the deficiency of middle element, the continuity of samples is cut off. Traditional SS technology cannot be used directly in the vector $\mathbf{r}$. Hence, we can only use the PSS technology to deal with this vector. Denote vector $\tilde{\mathbf{r}}_k$ and matrix $\tilde{\mathbf{B}}_k$ as

$$\tilde{\mathbf{r}}_k = \begin{bmatrix} \mathbf{r}_{1k} \\ \mathbf{r}_{-1k} \end{bmatrix}, \quad k = 1, 2, \ldots, K \tag{6}$$

and

$$\tilde{\mathbf{B}}_k = \begin{bmatrix} \mathbf{B}_{1k} \\ \mathbf{B}_{-1k} \end{bmatrix}, \quad k = 1, 2, \ldots, K \tag{7}$$

where $\mathbf{r}_{1k} = \mathbf{r}_1(k : F - K + k)$, $\mathbf{r}_{-1k} = \mathbf{r}_{-1}(k : F - K + k)$, $\mathbf{B}_{1k} = \mathbf{B}_1(k : F - K + k, :)$ and $\mathbf{B}_{-1k} = \mathbf{B}_{-1}(k : F - K + k, :)$.

Since the two sub-manifold matrices $\mathbf{B}_1$ and $\mathbf{B}_{-1}$ still correspond to two independent hole-free virtual arrays, $\tilde{\mathbf{B}}_k$ and $\tilde{\mathbf{B}}_1$ satisfy the equation

$$\tilde{\mathbf{B}}_k = \tilde{\mathbf{B}}_1 \Psi^{k-1} \tag{8}$$

where $\tilde{\mathbf{B}}_1 = [\ \mathbf{B}_{11}^T \quad \mathbf{B}_{-11}^T\ ]^T$, $\mathbf{B}_{11} = [\mathbf{b}_{11}(\theta_1), \mathbf{b}_{11}(\theta_2), \ldots, \mathbf{b}_{11}(\theta_K)]$ with $\mathbf{b}_{11}(\theta_k) = [e^{\frac{j2\pi dF \sin\theta_k}{\lambda}}, e^{\frac{j2\pi d(F-1)\sin\theta_k}{\lambda}}, \ldots, e^{\frac{j2\pi K \sin\theta_k}{\lambda}}]^T$, $\mathbf{B}_{-11} = [\mathbf{b}_{-11}(\theta_1), \mathbf{b}_{-11}(\theta_2), \ldots, \mathbf{b}_{-11}(\theta_K)]$ with $\tilde{\mathbf{b}}_{-11}(\theta_k) = [e^{-\frac{j2\pi \sin\theta_k}{\lambda}}, \ldots, e^{-\frac{j2\pi(F-K+1)\sin\theta_k}{\lambda}}]^T$, $\Psi = \mathrm{diag}\{e^{-\frac{j2\pi \sin\theta_1}{\lambda}}, e^{-\frac{j2\pi \sin\theta_2}{\lambda}}, \ldots, e^{-\frac{j2\pi \sin\theta_K}{\lambda}}\}$.

From Eqs. (6) and (8), $\tilde{\mathbf{r}}_k$ can be expressed as

$$\tilde{\mathbf{r}}_k = \tilde{\mathbf{B}}_k \mathbf{P} = \tilde{\mathbf{B}}_1 \Psi^{k-1} \mathbf{P} \tag{9}$$

Being similar to [18, 21, 25], denote a partitioned matrix $\tilde{\mathbf{R}}$ as

$$\begin{aligned}
\tilde{\mathbf{R}} &= [\ \tilde{\mathbf{r}}_1 \quad \tilde{\mathbf{r}}_2 \quad \ldots \quad \tilde{\mathbf{r}}_K\ ] \\
&= [\ \tilde{\mathbf{B}}_1 \mathbf{P} \quad \tilde{\mathbf{B}}_1 \Psi \mathbf{P} \quad \ldots \quad \tilde{\mathbf{B}}_1 \Psi^{K-1} \mathbf{P}\ ] \\
&= \tilde{\mathbf{B}}_1 \mathbf{W}
\end{aligned} \tag{10}$$

where $\mathbf{W} = [\ \mathbf{P} \quad \Psi\mathbf{P} \quad \ldots \quad \Psi^{K-1}\mathbf{P}\ ]$. It is easy to know that $\mathbf{W}$ is a K-order invertible matrix as [21, 25].

In fact, since $\mathbf{W}$ in Eq. (10) is an invertible matrix, $\tilde{\mathbf{R}}$ can be seen as a signal subspace which corresponds to the manifold matrix $\tilde{\mathbf{B}}_1$. Because the manifold matrix $\tilde{\mathbf{B}}_1$ does not belong to a hole-free virtual array, $\tilde{\mathbf{R}}$ can only be seen as an incomplete signal subspace. In this case, if MUSIC algorithm or ESPRIT algorithm is used to deal with $\tilde{\mathbf{R}}$ directly, it is difficult to get precise DOA estimation. Only when $\tilde{\mathbf{R}}$ is repaired into a complete signal subspace, high precision DOA estimation can be obtained in MUSIC algorithm or ESPRIT algorithm.

4.2. Repair of Signal Subspace

Although $\tilde{\mathbf{B}}_1$ does not belong to a hole-free virtual array, it is shown that the two sub-matrices $\mathbf{B}_{11}$ and $\mathbf{B}_{-11}$ correspond to two virtual arrays with consecutive virtual sensors. For taking the advantage of this property, $\tilde{\mathbf{R}}$ is partitioned into

$$\tilde{\mathbf{R}} = \begin{bmatrix} \tilde{\mathbf{R}}_1 \\ \tilde{\mathbf{R}}_{-1} \end{bmatrix} \tag{11}$$

where $\tilde{\mathbf{R}}_1 = \mathbf{B}_{11}\mathbf{W} \in C^{(F-K+1)\times K}$ and $\tilde{\mathbf{R}}_{-1} = \mathbf{B}_{-11}\mathbf{W} \in C^{(F-K+1)\times K}$.

Then, six matrices, $\tilde{\mathbf{R}}_{11} \in C^{(F-K)\times K}$, $\tilde{\mathbf{R}}_{12} \in C^{(F-K)\times K}$, $\tilde{\mathbf{R}}_{13} \in C^{K\times K}$, $\tilde{\mathbf{R}}_{-11} \in C^{(F-K)\times K}$, $\tilde{\mathbf{R}}_{-12} \in C^{(F-K)\times K}$, and $\tilde{\mathbf{R}}_{-13} \in C^{(K-1)\times K}$, are extracted from $\tilde{\mathbf{R}}_1$ and $\tilde{\mathbf{R}}_{-1}$ by

$$\begin{cases} \tilde{\mathbf{R}}_{11} = \tilde{\mathbf{R}}_1(1:F-K,:) \\ \tilde{\mathbf{R}}_{12} = \tilde{\mathbf{R}}_1(2:F-K+1,:) \\ \tilde{\mathbf{R}}_{13} = \tilde{\mathbf{R}}_1(F-2K+2:F-K+1,:) \\ \tilde{\mathbf{R}}_{-11} = \tilde{\mathbf{R}}_{-1}(1:F-K,:) \\ \tilde{\mathbf{R}}_{-12} = \tilde{\mathbf{R}}_{-1}(2:F-K+1,:) \\ \tilde{\mathbf{R}}_{-13} = \tilde{\mathbf{R}}_{-1}(F-2K+3:F-K+1,:) \end{cases} \tag{12}$$

According to Eqs. (10), (11), and (12), the six sub-matrices can be written as

$$\begin{cases} \tilde{\mathbf{R}}_{11} = \mathbf{B}_{11}(1:F-K,:)\mathbf{W} \\ \tilde{\mathbf{R}}_{12} = \mathbf{B}_{11}(2:F-K+1,:)\mathbf{W} \\ \tilde{\mathbf{R}}_{13} = \mathbf{B}_{11}(F-2K+2:F-K+1,:)\mathbf{W} \\ \tilde{\mathbf{R}}_{-11} = \mathbf{B}_{-11}(1:F-K,:)\mathbf{W} \\ \tilde{\mathbf{R}}_{-12} = \mathbf{B}_{-11}(2:F-K+1,:)\mathbf{W} \\ \tilde{\mathbf{R}}_{-13} = \mathbf{B}_{-11}(F-2K+3:F-K+1,:)\mathbf{W} \end{cases} \tag{13}$$

Continue to construct two block matrices $\widehat{\mathbf{R}}_1 = [\ \tilde{\mathbf{R}}_{11}^T \quad \tilde{\mathbf{R}}_{-11}^T\ ]^T \in C^{2(F-K)\times K}$, $\widehat{\mathbf{R}}_2 = [\ \tilde{\mathbf{R}}_{12}^T \quad \tilde{\mathbf{R}}_{-12}^T\ ]^T \in C^{2(F-K)\times K}$, and the two matrices have the relationship

$$\begin{aligned} \widehat{\mathbf{R}}_2 &= \left[\begin{array}{c} \mathbf{B}_{11}(2:F-K+1,:) \\ \mathbf{B}_{-11}(2:F-K+1,:) \end{array} \right] \mathbf{W} \\ &= \left[\begin{array}{c} \mathbf{B}_{11}(1:F-K,:) \\ \mathbf{B}_{-11}(1:F-K,:) \end{array} \right] \Psi\mathbf{W} \\ &= \widehat{\mathbf{R}}_1\Psi\mathbf{W} \end{aligned} \tag{14}$$

From Eq. (14), it is easy to know

$$\widehat{\mathbf{R}}_1^{+}\widehat{\mathbf{R}}_2 = \mathbf{W}^{-1}\Psi\mathbf{W} \tag{15}$$

Like ESPRIT algorithm [23], we can get the estimations of DOAs by EVD of $\widehat{\mathbf{R}}_1^{+}\widehat{\mathbf{R}}_2$. If this is done, only the partial completeness of $\tilde{\mathbf{R}}$ is utilized. Obviously, it is almost impossible to get satisfactory estimation results.

For repairing the incomplete signal subspace $\tilde{\mathbf{R}}$, $\widehat{\mathbf{R}}_1^{+}\widehat{\mathbf{R}}_2$ is used to construct two matrices $\tilde{\mathbf{R}}_1' = \tilde{\mathbf{R}}_{13}(\widehat{\mathbf{R}}_1^{+}\widehat{\mathbf{R}}_2)^K \in C^{K\times K}$ and $\tilde{\mathbf{R}}_{-1}' = \tilde{\mathbf{R}}_{-13}(\widehat{\mathbf{R}}_1^{+}\widehat{\mathbf{R}}_2)^{K-1} \in C^{(K-1)\times K}$. According to Eq. (15), $\tilde{\mathbf{R}}_1'$ and $\tilde{\mathbf{R}}_{-1}'$ have the other forms

$$\begin{aligned} \tilde{\mathbf{R}}_1' &= \mathbf{B}_{11}(F-2K+2:F-K+1,:)\mathbf{W}(\mathbf{W}^{-1}\Psi\mathbf{W})^K \\ &= \mathbf{B}_{11}(F-2K+2:F-K+1,:)\Psi^K\mathbf{W} \\ &= \mathbf{B}_{11}'\mathbf{W} \end{aligned} \tag{16}$$

and

$$\begin{aligned} \tilde{\mathbf{R}}_{-1}' &= \mathbf{B}_{-11}(F-2K+3:F-K+1,:)\mathbf{W}(\mathbf{W}^{-1}\Psi\mathbf{W})^{K-1} \\ &= \mathbf{B}_{-11}(F-2K+3:F-K+1,:)\Psi^{K-1}\mathbf{W} \\ &= \mathbf{B}_{-11}'\mathbf{W} \end{aligned} \tag{17}$$

where $\mathbf{B}_{11}'$ can be expressed in detail as $\mathbf{B}_{11}' = [\mathbf{b}_{11}'(\theta_1), \mathbf{b}_{11}'(\theta_2), \ldots, \mathbf{b}_{11}'(\theta_K)]$ with $\mathbf{b}_{11}'(\theta_k) = [e^{\frac{j2\pi d(K-1)\sin\theta_k}{\lambda}}, \ldots, e^{\frac{j2\pi d\sin\theta_k}{\lambda}}, 1]^T$, and $\mathbf{B}_{-11}'$ can be expressed in detail as $\mathbf{B}_{-11}' = [\mathbf{b}_{-11}'(\theta_1), \mathbf{b}_{-11}'(\theta_2), \ldots, \mathbf{b}_{-11}'(\theta_K)]$ with $\mathbf{b}_{-11}'(\theta_k) = [e^{-\frac{j2\pi(F-K+2)\sin\theta_k}{\lambda}}, \ldots, e^{-\frac{j2\pi F\sin\theta_k}{\lambda}}]^T$.

Observing the property of $\mathbf{B}_{11}$, $\mathbf{B}'_{11}$, $\mathbf{B}_{-11}$, and $\mathbf{B}'_{-11}$, it is easy to know that $\mathbf{B} = \begin{bmatrix} (\mathbf{B}_{11})^T & (\mathbf{B}'_{11})^T & (\mathbf{B}_{-11})^T & (\mathbf{B}'_{-11})^T \end{bmatrix}^T \in C^{(2F+1)\times K}$. According to this relationship, we denote a new partitioned matrix $\mathbf{R}_{new} = \begin{bmatrix} (\tilde{\mathbf{R}}_1)^T & (\tilde{\mathbf{R}}'_1)^T & (\tilde{\mathbf{R}}_{-1})^T & (\tilde{\mathbf{R}}'_{-1})^T \end{bmatrix}^T \in C^{(2F+1)\times K}$.

According to Eqs. (16) and (17), we can know

$$\mathbf{R}_{new} = \begin{bmatrix} \tilde{\mathbf{R}}_1 \\ \tilde{\mathbf{R}}'_1 \\ \tilde{\mathbf{R}}_{-1} \\ \tilde{\mathbf{R}}'_{-1} \end{bmatrix} = \begin{bmatrix} \mathbf{B}_{11}\mathbf{W} \\ \mathbf{B}'_{11}\mathbf{W} \\ \mathbf{B}_{-11}\mathbf{W} \\ \mathbf{B}'_{-11}\mathbf{W} \end{bmatrix} = \mathbf{BW} \tag{18}$$

From Eq. (18), it is obvious that $\mathbf{R}_{new}$ is a complete signal subspace. At this point, we can deal with $\mathbf{R}_{new}$ directly to get high-precision and unambiguous DOA estimations in MUSIC algorithm [22] or ESPRIT algorithm [23]. We should also mention that ESPRIT algorithm [23] can be used indiscriminately. But for MUSIC algorithm, we need to maximize the function $f(\theta)$ as [25]

$$f(\theta) = \frac{1}{\mathbf{b}^H(\theta)(\mathbf{I} - \mathbf{R}_{newo}\mathbf{R}_{newo}^H)\mathbf{b}(\theta)} \tag{19}$$

where $\mathbf{R}_{newo}$ is the Smith orthonormalization of $\mathbf{R}_{new}$. We should state that the function $f(\theta)$ is given by reference to [25]. For avoiding redundancy, we did not give the derivation on the orthogonality of $\mathbf{b}(\theta_k)$ and $\mathbf{I} - \mathbf{R}_{newo}\mathbf{R}_{newo}^H$.

Seeing the process of constructing complete signal subspace $\mathbf{R}_{new}$ from Eqs. (11) to (18), we can know that no EVD needs to be performed.

5. COMPLEXITY ANALYSIS

In this section, we compare the complexity of SS algorithm with the proposed PSS algorithm. The main difference of two spatial smoothing methods is concentrated on obtaining signal subspace or noise subspace. After the signal subspace or noise subspace is acquired, many common approaches can be used to estimate the DOA. Hence, we only compare the computational complexity of the two spatial smoothing methods in estimating signal subspace or noise subspace. Still suppose that the number of DOFs of a sparse MIMO is $2F + 1$ and that the number of snapshots is T. The main computational complexities of SS algorithm and proposed PSS algorithm are $O\{(2F + 1)T + (F + 1)^3\}$ and $O\{2FT\}$, respectively. Obviously, the proposed PSS algorithm has lower computational complexity than SS algorithm.

6. SIMULATION

In this section, we test the performance of proposed PSS algorithm by carrying out several groups of simulation experiments. Because the DOF of a nested MIMO radar is higher than a co-prime MIMO radar, we only consider that a nested MIMO radar [19] and an improved nested MIMO radar [20] are used for DOA estimation. Both employed MIMO radars consist of a 4-element transmitting array and a 4-element receiving array as shown in Fig. 1 and Fig. 2. Suppose that $\tilde{\mathbf{R}}$ is constructed according to Eq. (10), and $\mathbf{R}''_{xx}$ is used for the traditional SS algorithm. Evaluation index of DOA estimation accuracy is root mean square error (RMSE), which is expressed as

$$RMSE = \sqrt{\frac{1}{KJ}\sum_{j=1}^{J}\sum_{k=1}^{K}(\hat{\theta}_{kj} - \theta_k)^2} \tag{20}$$

where $J = 500$ is the number of repetitive experiments in the same condition, and $\hat{\theta}_{kj}$ is the estimation of θ_k in the jth repetitive experiment. We select the MUSIC algorithm to estimate the DOA after obtaining the signal subspace or noise subspace by PSS algorithm or SS algorithm.

In the first set of experiments, we test the spatial spectrums of SS algorithm and PSS algorithm in two nested MIMO radar arrays. Suppose that the number of snapshots is 500 and that SNR is 5 dB.
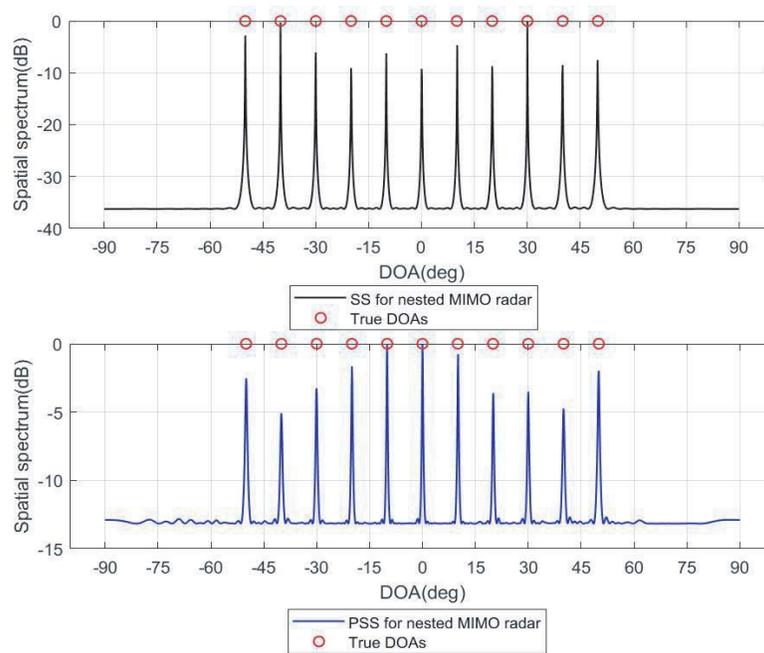
Figure 3. Spatial spectrums of nested MIMO radar.
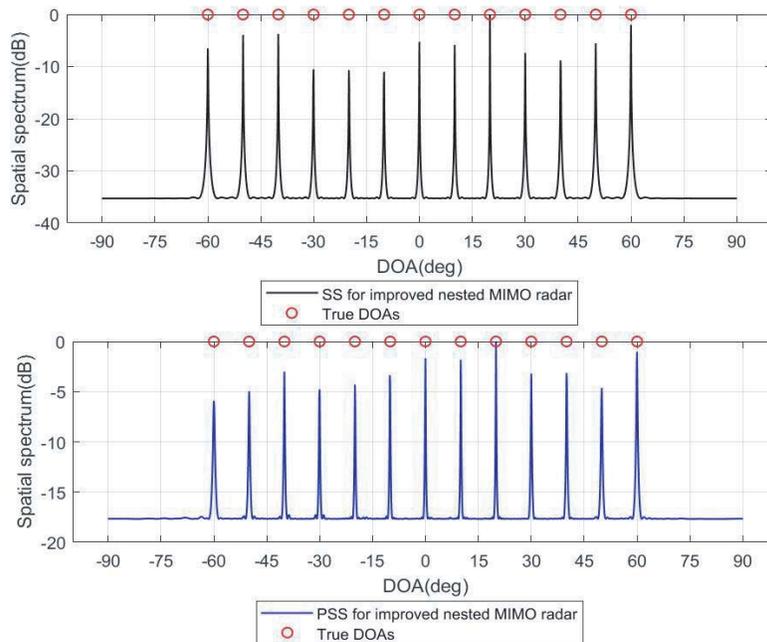

Figure 4. Spatial spectrums of improved nested MIMO radar.

Fig. 3 shows the spatial spectrums of SS algorithm and PSS algorithm for the nested MIMO radar arrays [19]. The DOAs of 11 targets are $-50°$, $-40°$, $-30°$, $-20°$, $-10°$, $0°$, $10°$, $20°$, $30°$, $40°$, $50°$, respectively. Fig. 4 shows the spatial spectrums of SS algorithm and PSS algorithm for the improved nested MIMO radar arrays [20]. The DOAs of 13 targets are $-60°$, $-50°$, $-40°$, $-30°$, $-20°$, $-10°$, 0, $10°$, $20°$, $30°$, $40°$, $50°$, and $60°$, respectively. The presentation shown in Fig. 3 and Fig. 4 can illustrate that both the SS algorithm and PSS algorithm have satisfactory angle resolution. Hence, these results can also preliminarily demonstrate the feasibility of proposed PSS algorithm.

In the second set of experiments, the comparison of RMSE is shown to further prove the performance of proposed PSS algorithm. Suppose that the DOAs of 8 targets are $60°$, $-50°$, $-30°$, $-10°$, $0°$, $20°$, $40°$, $60°$, respectively. Fig. 5 shows the RMSE of different algorithms versus SNR with 500 snapshots. Fig. 6 shows the RMSE of different algorithms versus snapshots with 5 dB SNR. From Fig. 5 and Fig. 6, we can see clearly that the proposed PSS has higher estimation precision than SS, no matter what kind of nested MIMO radar. The accuracy of a space-based algorithm is related to the number of rows of the signal subspace. In these experiments, for the proposed PSS algorithm, the number of rows of the repaired signal subspace $\mathbf{R}_{new}$ is larger than the signal subspace got by EVD of $\mathbf{R}''_{xx}$. In this case, it is reasonable to arrive at such results.
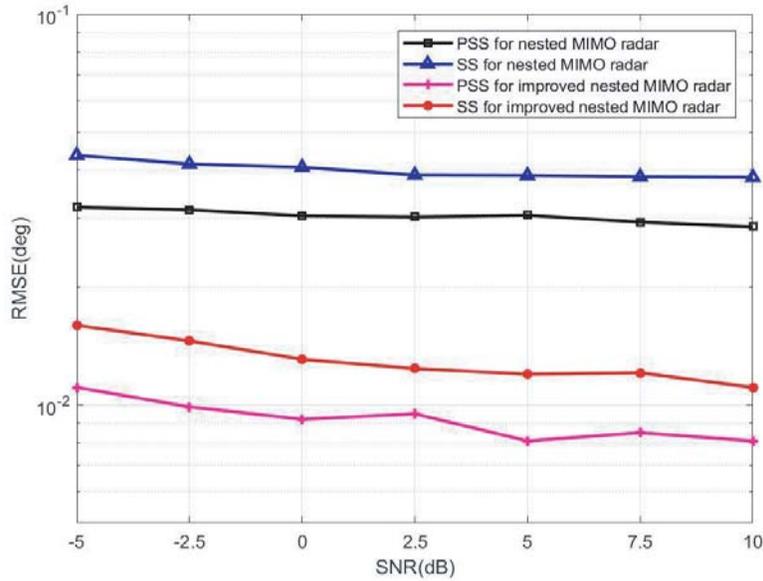

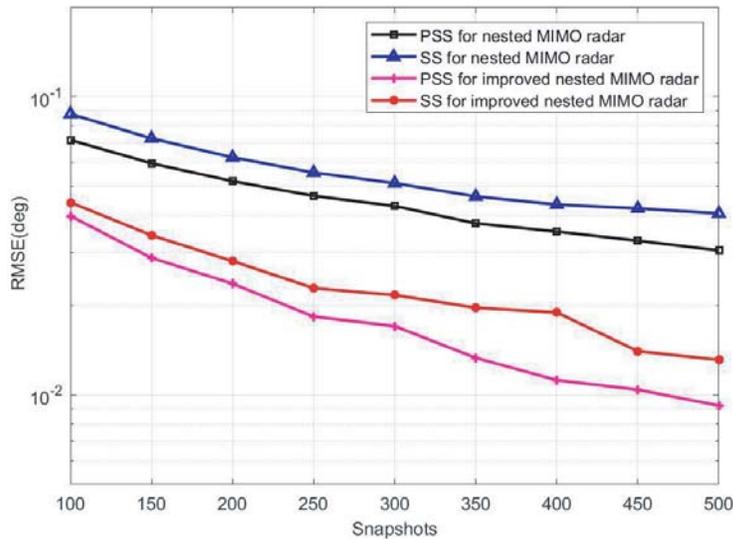
Figure 5. Comparsion of RMSE versus SNR.

Figure 6. Comparison of RMSE versus snapshots.

7. CONCLUSION

For the purpose of reducing the complexity of sparse MIMO radar in DOA estimation, this paper proposes a PSS algorithm based on the traditional SS algorithm. Being different from SS algorithm, PSS algorithm can get the complete signal subspace without EVD. Complexity analysis proves that the proposed PSS algorithm needs less calculated amount than SS algorithm to get the signal subspace. Two kinds of nested MIMO radars are used to test the performance of proposed algorithm. Simulation results show that the proposed PSS algorithm has higher estimation precision than SS. Hence, the proposed method may be a reference to the direction-finding in sparse MIMO radar.

ACKNOWLEDGMENT

REFERENCES

1. Liu, S., J. Zhao, and W. Li, "Subspace extension algorithm for joint DOA and DOD estimation in bistatic MIMO radar," *International Conference on Artificial Intelligence and Security*, 244–252, Springer, Cham, 2019.

2. Xia, T. Q., "Joint diagonalization based DOD and DOA estimation for bistatic MIMO radar," *Signal Processing*, Vol. 108, 159–166, 2015.

3. Zheng, G. M. and B. X. Chen, "Unitary dual-resolution ESPRIT for joint DOD and DOA estimation in bistatic MIMO radar," *Multidimensional Systems and Signal Processing*, Vol. 26, No. 1, 159–178, 2015.

4. Qi, H., H. Jiang, and S. Yao, "Joint multi-target DOD and DOA estimation in bistatic MIMO radar exploiting 2-level nested arrays," *International Conference on Radar Systems (Radar 2017)*, 1–4, IET, Belfast, UK, 2017.

5. Zheng, Z. and J. Zhang, "Fast method for multi-target localisation in bistatic MIMO radar," *Electronics Letters*, Vol. 47, 138–139, 2011.

6. Gao, H., J. Li, and M. Diao, "Direction finding of bistatic MIMO radar based onquantum-inspired grey wolf optimization in the impulse noise," *EURASIP Journal on Advances in Signal Processing*, Vol. 2018, 1–14, 2018.

7. Xie, R., Z. Liu, and Z. J. Zhang, "DOA estimation for monostatic MIMO radar using Polynomial root," *Signal Processing*, Vol. 90, No. 12, 3284–3288, 2010.

8. Zhang, X. and D. Xu, "Low-complexity ESPRIT-based DOA estimation for collocated MIMO radar," *Electronic Letters*, Vol. 47, No. 4, 283–284, 2011.

9. Zhang, X., Y. Huang, C. Chen, and D. Xu, "Reduced-complexity Capon for direction of arrival estimation in a monostatic multiple-input multiple-output radar," *IET Radar, Sonar and Navigation*, Vol. 6, No. 8, 796–801, 2012.

10. Li, J. F., X. F. Zhang, W. Y. Chen, and T. Hu, "Reduced-Dimensional ESPRIT for direction finding in monostatic MIMO radar with double parallel uniform linear arrays," *Wireless Personal Communication*, Vol. 77, No. 1, 1–19, 2014.

11. Wang, W., X. P. Wang, H. G. Song, and Y. H. Ma, "Conjugate ESPRIT for DOA estimation in monostatic MIMO radar," *Signal Processing*, Vol. 93, No. 7, 2070–2075, 2013.

12. Shi, J., G. Hu, X. Zhang, and Y. Xiao, "Symmetric sum coarray based co-prime MIMO configuration for direction of arrival estimation," *AEU-International Journal of Electronics and Communications*, Vol. 94, 339–347, 2018.

13. Shi, J., G. Hu, and X. Zhang, "Generalized co-prime MIMO radar for DOA estimation with enhanced degrees of freedom," *IEEE Sensors Journal*, Vol. 18, No. 3, 1203–1212, 2018.

14. Vaidyanathan, P. P. and P. Pal, "Sparse sensing with co-prime samplers and arrays," *IEEE Transactions on Signal Processing*, Vol. 59, No. 2, 573–586, 2011.

15. Pal, P. and P. P. Vaidyanathan, "Coprime sampling and the MUSIC algorithm," *Proceedings of Digital Signal Processing Workshop and IEEE Signal Processing Education Workshop (DSP/SPE)*, 289–294, Sedona, AZ, USA, 2011.

16. Pal, P. and P. P. Vaidyanathan, "Nested arrays: A novel approach to array processing with enhanced degrees of freedom," *IEEE Transactions on Signal Processing*, Vol. 58, No. 8, 4167–4181, 2010.

17. Yang, M., L. Sun, X. Yuan, and B. Chen, "Improved nested array with hole-free DCA and more degrees of freedom," *Electronics Letters*, Vol. 52, No. 25, 2068–2070, 2016.

18. Liu, S., Q. Liu, J. Zhao, and Z. Yuan, "Triple two-level nested array with improved degrees of freedom," *Progress In Electromagnetics Research B*, Vol. 84, 135–151, 2019.

19. Yang, M., L. Sun, X. Yuan, and B. Chen, "A new nested MIMO array with increased degrees of freedom and hole-free difference coarray," *IEEE Signal Processing Letters*, Vol. 25, No. 1, 40–44, 2018.

20. Liu, Q., B. Wang, X. Li, J. Tian, T. Cheng, and S. Liu, "An optimizing nested MIMO array with hole-free 322 difference coarray," *MATEC Web of Conferences*, Vol. 232, 01055, EDP Sciences, 2018.

21. Gu, J. F., P. Wei, and H. M. Tai, "2-D direction-of-arrival estimation of coherent signals using cross-correlation matrix," *Signal Processing*, Vol. 88, 75–85, 2008.

22. Schmidt, R. O., "Multiple emitter location and signal parameter estimation," *IEEE Transactions on Antennas Propagation*, Vol. 34, No. 3, 276–280, 1986.

23. Richard, R. and T. Kailath, "ESPRIT-estimation of signal parameters via rotational invariance techniques," *IEEE Trans. Acous, Speech, and Signal Process.*, Vol. 37, No. 7, 984–995, 1989.

24. Marcos, S., Marsal, and A. Benidir, "The propagator method for source bearing estimation," *Signal Processing*, Vol. 42, No. 2, 121–138, 1995.

25. Nie, X. and L. P. Li, "A computationally efficient subspace algorithm for 2-D DOA estimation with L-shaped array," *IEEE Signal Processing Letters*, Vol. 21, No. 8, 971–974, 2014.